



Simulations of an Experimental Centerbody-less Rotating Detonation Combustor

Douglas A. Schwer¹

Ryan Johnson²

*Laboratories for Computational Physics and Fluid Dynamics
Naval Research Laboratory, Washington, DC 20375*

Ephraim Gutmark³

*Department of Aerospace Engineering and Engineering Mechanics
University of Cincinnati, Cincinnati, OH 45221-0070*

Abstract

This paper presents results of a simulation for a centerbody-less rotating detonation combustor (RDC) rig from University of Cincinnati. The non-premixed hollow RDC simulation showed a stable detonation running an ethylene/air mixture with a mass-flow rate of 0.647 kg/s and an equivalence ratio of 1.12. Fuel injection was through discrete axial injectors with a radially inward air slot injection. The injection pattern produced two recirculation zones, a small one near the injectors on the outside wall, and a second recirculation zone further into the fill region. Three regions of heat-release related to the detonation wave were identified: the upper portion of the detonation wave, which was the strongest with heat release extending slightly into the interior of the domain, a region that hugged the wall and showed a somewhat corrugated presentation on the outer wall due to the discrete fuel injection, and a third region near the injectors that lagged the other two. The presence of strong heat-release lagging the main detonation wave resulted in an additional reflected shock wave running parallel to the oblique shock wave from the top of the detonation, which was consistent with earlier simulations using an ideal injection model. This solution demonstrated the potential of simulations to help understand the dynamics underlying hollow RDCs.

I. Introduction

ENGINES based on the higher thermodynamic efficiency of the detonation cycle have long been an attractive target for advanced propulsion concepts, but the unsteady nature of the detonation wave along with high pressure pulses, heat transfer rates, and highly non-linear detonation wave dynamics have made realizing the potential of the detonation cycle challenging. Over the last decade, there has increasing interest in rotating detonation engines (RDEs), which currently hold the most promise to realize the potential of the detonation cycle¹. There have been an extensive number of experimental, numerical, and theoretical studies on RDEs.

The conventional RDE has an annular combustion chamber with inner and outer walls. Both walls serve as reflecting surfaces for the detonation wave, stabilizing the detonation and also, for small differences in radii, making the flow quasi-two-dimensional. However, for an engine, they also add structural elements to the engine that require cooling and create viscous boundary layers, and thus losses. For this reason, some investigators have examined removing the inner wall and getting rid of the centerbody altogether. These hollow-RDEs replace the centerbody typically with a head-end wall creating a large dump region in the center portion of the engine. Injection of the fresh premixture

¹ Mechanical Engineer, Code 6041, Naval Research Laboratory, AIAA Senior Member.

² Research Engineer, Code 6041, Naval Research Laboratory, AIAA Member.

³ Distinguished Professor, University of Cincinnati, AIAA Fellow.

still occurs in an annular ring near the outer diameter such that the detonation wave still rotates around the outer wall. Early numerical work²⁻⁴ showed this was possible, while some more recent experimental work^{5,6} have suggested that not only does removing the centerbody help reduce the mass and cooling requirements of the RDE, but also improves the detonative properties. Reference 6 authors have used a frequency analysis technique to calculate detonation velocities that approach $0.95 D_{cj}$, which is considerably higher than typical RDEs. Their reasoning is that by removing the viscous losses associated with the inner wall, the detonation wave becomes more efficient. In addition to that, numerical work² has shown that hollow RDC's provide similar performance as their annular brethren.

Numerical results and analysis from References 2 and 3 have shed considerable light on the basic dynamics of hollow RDEs. Work from Tang² described the basic dynamics of a hollow RDE with a large injection surface (corresponding to an annular RDE with a large difference in inner and outer diameters). Results showed they recovered similar mass flow rates as the annular RDE with the same injection surface area and length, and produced about 90% of the thrust and thus Isp. Further studies by Yao³ showed that performance improved as the ratio of injection surface area to total head-end area was increased, although this improvement was relatively small and resulting in efficiencies still smaller than the annular RDE results. Their calculations did not consider drag and heat loss to the inner wall, which will likely bring down the performance of annular RDEs, but have less of an effect on the hollow RDEs. Our recent work for a small (100 mm outer diameter and length) RDC in annular, hollow, and flow-through configurations is consistent with the previous results⁷. The injection surface and manifold conditions were kept the same for the different configurations. The radial depth (difference between the outer and inner radius of the injection surface) was similar to current annular RDC rigs. Results showed that the net thrust dropped by almost 50% for the hollow RDC, but recovered for some of the flow-through configurations. Furthermore, all of the centerbody-less RDC simulations showed large areas of low velocity within the exhaust plane of the combustor. Further investigations (not included in the paper) showed that for larger injection surfaces (that is, a larger radial depth for annular RDCs), the performance dramatically improves and the large area of low velocity in the exhaust plane becomes smaller, similar to other numerical results^{2,3}. This was addressed in a follow on paper⁸, where we studied the addition of a convergent divergent section to a centerbody-less RDE, and used area ratios, mass-flow rates and injection areas that were based on a design for a ram RDE concept. Optimized shaping of the combustion chamber and nozzle were not considered for this paper, but it represents a more honest assessment of the propulsive capabilities of these devices than the more simple cylindrical geometries initially considered.

Through the two previous papers^{7,8}, stability issues were not specifically addressed as the results focused more on the flow-field characteristics and efficiency of a stable running centerbody-less RDEs. Because of the loss of the reflecting surface from an inner wall, the detonation waves in these devices may be more susceptible to detonation failure than annular RDEs. However, RDEs have been surprisingly stable for a wide variety of conditions. It has been postulated that reflecting surfaces provided by the injection system, along with the turbulence that occurs upstream of the detonation wave as reactants are being injected and mixed into the combustion chamber, provide enough opportunities for focusing pressure waves such that the normal transverse wave structures created from reflections off of walls are not required in the same way as they are in a detonation tube. For the ideal injection surface used in our previous papers, we used a fast-reacting chemical mechanism that ensured stable detonation.

For this paper, we begin to address the stability behavior associated with a centerbody-less RDE design, and ground our computations with experiments being conducted at the University of Cincinnati. Our aim is to better understand how the detonation mechanism behaves for centerbody-less RDEs, and how they differ from what we understand in annular RDEs. Experimental validation of these results will be an important aspect of the study, since detailed kinetics and resolution needed to resolve these kinetics is still out of reach for computational codes. The experiments currently being

run at University of Cincinnati use a rig based on their earlier work⁶, with an updated injection system and the capability of flowing gases through the core region. We use the JENRE® Multiphysics Framework for doing our computations^{8,9}, which has been developed at NRL over the past several years to make use of GPU architectures for efficient computation.

II. Rotating Detonation Engine Model

For RDE calculations, the conservation equations solved are the multi-species, reacting Navier-Stokes equations with an additional equation for the induction parameter, τ :

$$\begin{aligned} \frac{\partial \rho}{\partial t} + \nabla \cdot \rho \mathbf{v} &= 0 \\ \frac{\partial \rho \mathbf{v}}{\partial t} + \nabla \cdot \rho \mathbf{v} \otimes \mathbf{v} &= -\nabla P - \nabla \cdot \mathbb{T}(\mu, \nabla \mathbf{v}) \\ \frac{\partial \rho e_t}{\partial t} + \nabla \cdot (\rho e_t + P) \mathbf{v} &= -\nabla \cdot \mathbf{q} - \nabla \cdot \mathbb{T}(\mu, \nabla \mathbf{v}) \cdot \mathbf{v} \\ \frac{\partial \rho Y_k}{\partial t} + \nabla \cdot \rho Y_k \mathbf{v} &= -\nabla \cdot \rho Y_k \mathbf{v}_k + \dot{\omega}_k \\ \frac{\partial \rho \tau}{\partial t} + \nabla \cdot \rho \tau \mathbf{v} &= \frac{\rho}{t_{ind}} \end{aligned}$$

Pressure and internal energy are calculated based on species densities and mixture temperature by $P = \sum_{k=1}^N \rho Y_k R_k T$, and $\rho e_t = \sum_{k=1}^N \rho Y_k u_k(T) + \frac{1}{2} \rho \mathbf{v} \cdot \mathbf{v}$. $u_k(T)$ is described by a curve-fit, and calculation of temperature requires an iterative procedure, but the curve-fit is well behaved and can be solved within a few iterations even with a poor initial guess for the temperature, T . We included an additional conserved variable, $\rho \tau$, along with the conserved gaseous state, which is used for induction-time parameter models (IPMs). We have written the transport terms in a very general sense as the viscous stress tensor, $\mathbb{T}(\mu, \nabla \mathbf{v})$ and the general heat flux, \mathbf{q} , which can be further divided into conduction, species transport, and radiation, and species diffusion velocities, \mathbf{v}_k . Currently the transport quantities are evaluated as mixture-averaged quantities of polynomial fits based on temperature. For this work, we are doing exclusively inviscid calculations due to the high speeds involved, however, the framework has been developed for viscous flows as well, and these terms will become important as we consider important processes such as injection and heat transfer in more detail for later work.

III. Solution Procedure

The conservation equations presented above are solved using the JENRE® Multiphysics Framework. This framework has been used for a number of detonation and high speed combustion studies^{7-9,15}. It implements all of these capabilities in C++ with extensive use of templates, so that the various physics, numerics, and mesh representation capabilities are implemented in a generic way, but are then combined at compile-time in order to ensure high efficiency. One of the overarching goals of the framework has been to achieve the highest computational performance possible while maintaining the flexibility to simulate geometrically and physically complex flow-fields. It implements both distributed memory and shared memory parallelism for modern CPU and GPU architectures^{ref.}.

The simulations accomplished for this paper use the continuous-Galerkin (CG) based solver developed as part of the JENRE® framework, which has been used extensively for jet noise calculations¹⁰. We use stationary grids for these calculations. The solver uses a stabilized Taylor-

Galerkin formulation with Flux-Corrected Transport (FCT) for handling shock waves and discontinuities. The shock capturing ensures monotonicity at shocks and sharp features.

IV. Results

All of the calculations target the hollow RDC geometry and conditions of the experimental rig at the University of Cincinnati. Their rig has a 154 mm outer diameter with radially inward slot air injection, and discrete axial fuel injectors. A cross-section of the overall geometry is shown in Figure 1 and relevant geometric parameters are given in Table 1. The simulations use ethylene as the fuel and air as the oxidizer. Experimental results have been obtained for this geometry for mass flow rates between 0.2 and 0.5 kg/s, and equivalence ratios between 0.5 and 1.5. More details of the configuration of which this is based is given in Ref. 6.

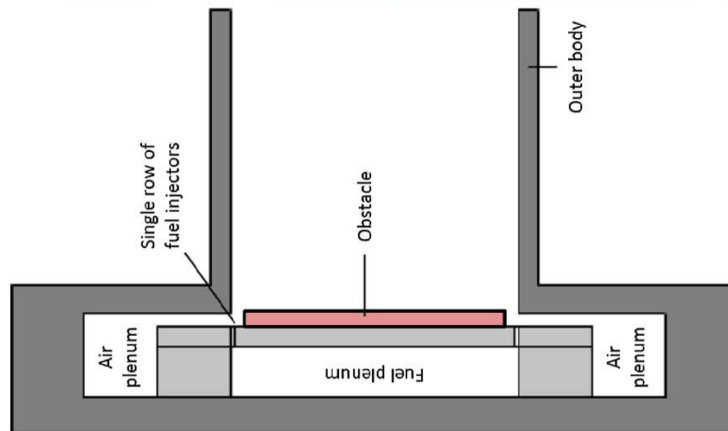


Figure 1. Cross section of hollow RDC geometry from University of Cincinnati [7].

Table 1. Hollow RDC sizing parameters

H-RDE Geom	
Length of chamber	131 mm
Outer diameter	154 mm
Diameter of circular obstacle	142 mm
Thickness of circular obstacle	3 mm
Diameter of row of fuel orifices	151 mm
Air inlet gap	0.5 mm
Fuel injector diameter	~0.765 mm
Number of fuel injectors	80

To do these simulations, we have created two meshes. One is a coarse mesh with ideal injection surfaces representing the feed system (thus, no fuel or air plenum or fuel injectors) and a large exhaust plenum. The exhaust plenum extends out to $10R$, thus 0.77 m, and 0.78 m past the exit of the combustor. The resolution for the detonation is 0.5 mm, and the inner core region has a resolution of 2 mm. The resultant mesh has 4.1 million points and 23.9 million tetrahedral elements. The second mesh is better resolved, and includes the injector and feed plenums shown in Figure 1 and described in Table 1. That mesh uses a 0.4 mm detonation resolution (still fairly coarse), and a 0.8 mm resolution for the core flow. Note that the resolution for the injectors becomes much finer than the 0.4 mm chamber resolution. The resultant mesh has 14.8 million points and 87.4 million elements. We use Capstone to generate the meshes[ref]. The full mesh and a closeup of the combustion chamber, injectors, and the top of the fuel and air feed plenums is shown in Figure 2.

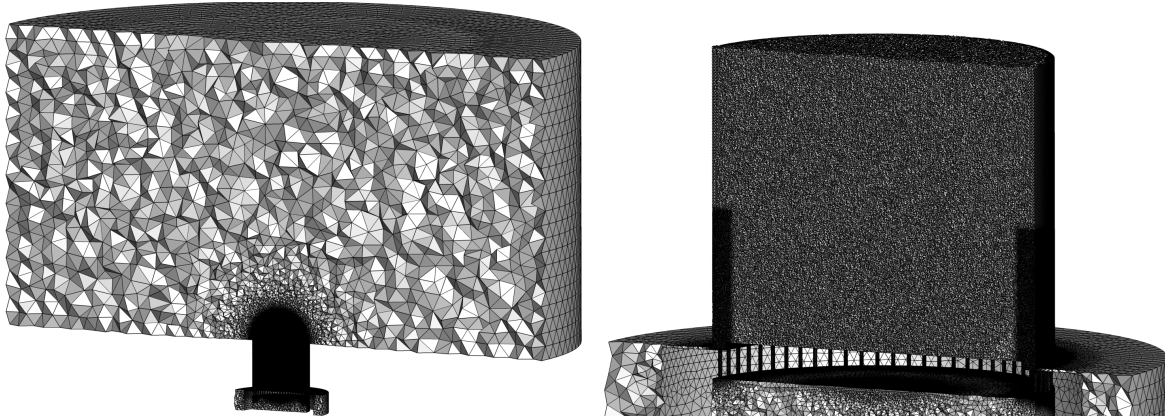


Figure 2. Total mesh for hollow RDC calculation (left), and closeup of combustion chamber (right).

Although there have been an extensive number of simulations for annular RDC rigs over the last several years, the number of hollow and flow-through RDC rig simulations has remained minimal. Several factors make the calculation of hollow RDCs more challenging than traditional annual RDCs, which are already very computationally intensive. First of all, the introduction of a dump region requires a large amount of additional meshing. Since shock waves may exist within the dump region, the meshing should be fine enough in this region to capture shock wave interactions. In addition, the dump region creates a large volume of fluid that interacts directly with the detonation wave. Because of the volume, it requires a large settling time, all while interacting with the detonation wave. Settling times for the detonation wave in annular RDCs rigs is already quite large (around 5 or 6 ms), especially if using a traditional start-up procedure with a high temperature, high pressure driver section. We get around this by using a staged start-up process. This is an artificial process, but the purpose is to speed up the settling time of the detonation wave and dump region by producing an initial condition on the mesh of interest that is closer to what we expect for the final solution.

In this way, we have been able to get stable solutions for a rotating detonation wave in a hollow-RDC rig for a mass-flow rate and overall equivalence ratio that is similar to that from experiments. Figure 3 shows the temperature and pressure of the outer wall and injection face. A stable detonation wave is seen running clockwise from right to left on the combustion wall. The mass flow rate of air is 0.60 kg/s for air, 0.047 kg/s for ethylene, which gives a global equivalence ratio of 1.16. The mass flow rate is about 20% higher than experiments, but still close to the target range. The appearance of the donation wave and the resultant dynamics are more complex than the ideal RDC calculation, and somewhat more complex than the RDC rig calculations. Part of this is due to the injectors, which can give a much more corrugated fill zone ahead of the detonation wave. But it is also interaction between the detonation wave and the dump region above the plug wall, as it interacts with the detonation wave. We discuss more about the shape of the pressure and temperature waves on the outer wall when we unroll the outer wall in Figure 6 and 7 below.

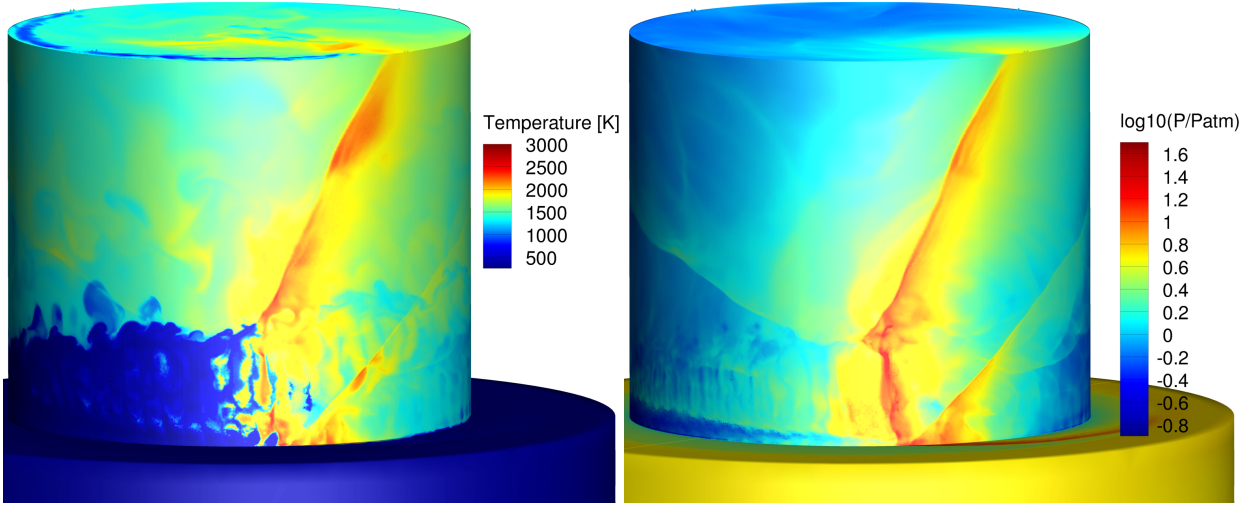


Figure 3. Temperature (left) and $\log_{10}(\text{pressure})$ (right) for the non-premixed H-RDE simulation based off of a University of Cincinnati rig [7]. $m = 0.647 \text{ kg/s}$, $\phi = 1.16$.

For non-premixed RDCs, mixing plays a critical role in the strength of the detonation wave and performance of the RDC. To quantify mixing here, we look at a quantity called mixing efficiency, or χ . The mixing efficiency is based on a global target equivalency ratio based on the mass flow rates of fuel and oxidizer into the feed plenums, and the local equivalency ratio at each point. For this calculation, we use a modified equivalence ratio, ϕ^* , defined below:

$$\phi^* \equiv \frac{2(F/O)}{(F/O) + (F/O)_{st}} = \frac{2F}{F + O(F/O)_{st}}$$

where F is the fuel and O is the oxidizer, and $(F/O)_{st}$ is the stoichiometric ratio of fuel to oxidizer. These terms can either be mass or mole based. We use this term because it is bounded for the pure fuel stream. $\phi^* = 0$ for pure oxidizer, $\phi^* = 2$ for pure fuel, and $\phi^* = 1$ for stoichiometric mixture (consistent with the normal equivalence ratio). Given the global ϕ_{gl}^* , we compute the mixing efficiency, χ , as:

$$\begin{aligned} \chi &\equiv \frac{\phi^* - \phi_{gl}^*}{2 - \phi_{gl}^*}, & \text{if } \phi^* > \phi_{gl}^* \\ &\equiv \frac{\phi_{gl}^* - \phi^*}{\phi_{gl}^*}, & \text{if } \phi^* < \phi_{gl}^* \end{aligned}$$

The mixing efficiency, χ , which shows how close or how far off we are to the target equivalency ratio. This gives us a local idea of mixing. We want to hit the sweet spot around 1 in the fill region, any value lower will be either fuel rich or lean. This value can be integrated to determine an overall mixing efficiency, but we have not done that for this case.

Figure 4 shows half of the combustor domain with injectors and the very top of the fuel and air feed plenums. Temperature, pressure, axial velocity, and the mixing efficiency is all plotted. This view also shows part of the flow-field in the dump region, which is a challenge to fully visualize. Temperature, as usual, shows the limit of the fill region very well. The reactant gases appear to hug the outer wall and then push inwards at the top of the fill zone. The pressure (or \log_{10} of the pressure) shows that pressures vary substantially in the core region, but directly above the fill region tend to be lower (possibly from acceleration of the fill reactants). The axial velocity shows two distinct recirculation regions near the injection. One recirculation (negative axial velocity) occurs near the fuel injectors and recirculates the fuel near the outer wall. The second is higher up and recirculates reactant inward near the top of the fill layer. Broader recirculation (negative axial velocity) is also found in the core region. The slow meandering of the core-flow is part of what

makes these simulations so difficult. We found this to be true in our previous studies of centerbody-less RDEs^{7,8}, and found that careful matching of the mass flow rates of the injectors and exit area is required to get better, more propulsive exhaust velocity. For these simulations, we are more interested in the stability of the detonation wave, and matching experimental conditions, so we will not focus on propulsive performance parameters. The mixing efficiency also clearly shows the fill zone in Fig. 4. The efficiency is highest right at the bottom of the detonation wave, and is much lower throughout much of the mixing zone. To determine where it is rich and lean, we would have to look at the equivalence ratio, ϕ^* , which is not shown here.

Figure 5 shows a surface contour of the heat-release, at 5×10^5 J/kg. This surface appears very noisy and is difficult to interpret, but this is the best way to visualize the detonation wave and its shape. To get a better sense of its three dimensional shape, we examine it from three different angles, from straight on (Fig 5a) to looking at it from 90 degrees (Fig. 5c). Looking at Fig. 5a, we can see that the wave has a slight lean to the towards the fill zone, and a fairly prominent region of combustion near the injectors but behind the detonation wave front. Examining Fig. 5c, we can see that it hugs the outer wall for most of the detonation wave, except towards the top of the wave, where it expands inward. The highest pressures also appear to develop in the top region of the detonation wave as well.

The outer wall can also be unrolled, which will give a good indication of how the fill zone, temperature, and pressure develops over a cycle. Figure 6 shows temperature, pressure, axial velocity, and mixing efficiency for the outer wall unrolled. As shown in Fig. 3 too, the temperature looks choppy right at the front of the detonation wave, and the pressure also shows some pre-detonation temperature and pressure rise. The pressure rise we believe is coming from the interior of the domain and is a common feature of the hollow geometries. This is pre-igniting some of the mixture, causing temperature rise and a smaller amount of pressure rise. The corrugations are due to the discrete injectors jets, where gas is being ignited between the jets, whereas the jets themselves are ignited in the detonation wave. The double oblique shock wave (or oblique shock wave and reflected wave) best seen in Fig. 6b and are labeled as features (A) and (B) is due to the heat-release near the injector plate lagging the heat-release higher up in the detonation wave. This feature was also seen in some previous work with ideal injectors, although in that case the detonation wave had a smooth front and not the corrugations seen here. This can also be clearly seen in the axial velocity, with the highest velocities just after both shock waves. Also shown in Fig. 6a-c is a reflection wave from the top of the detonation wave (feature C in Fig. 6b). In this case, it appears to anchor the top of the top of the detonation wave (feature D in Fig. 6b), although the authors are unsure if this is a coincidence or due to a resonance or forcing.

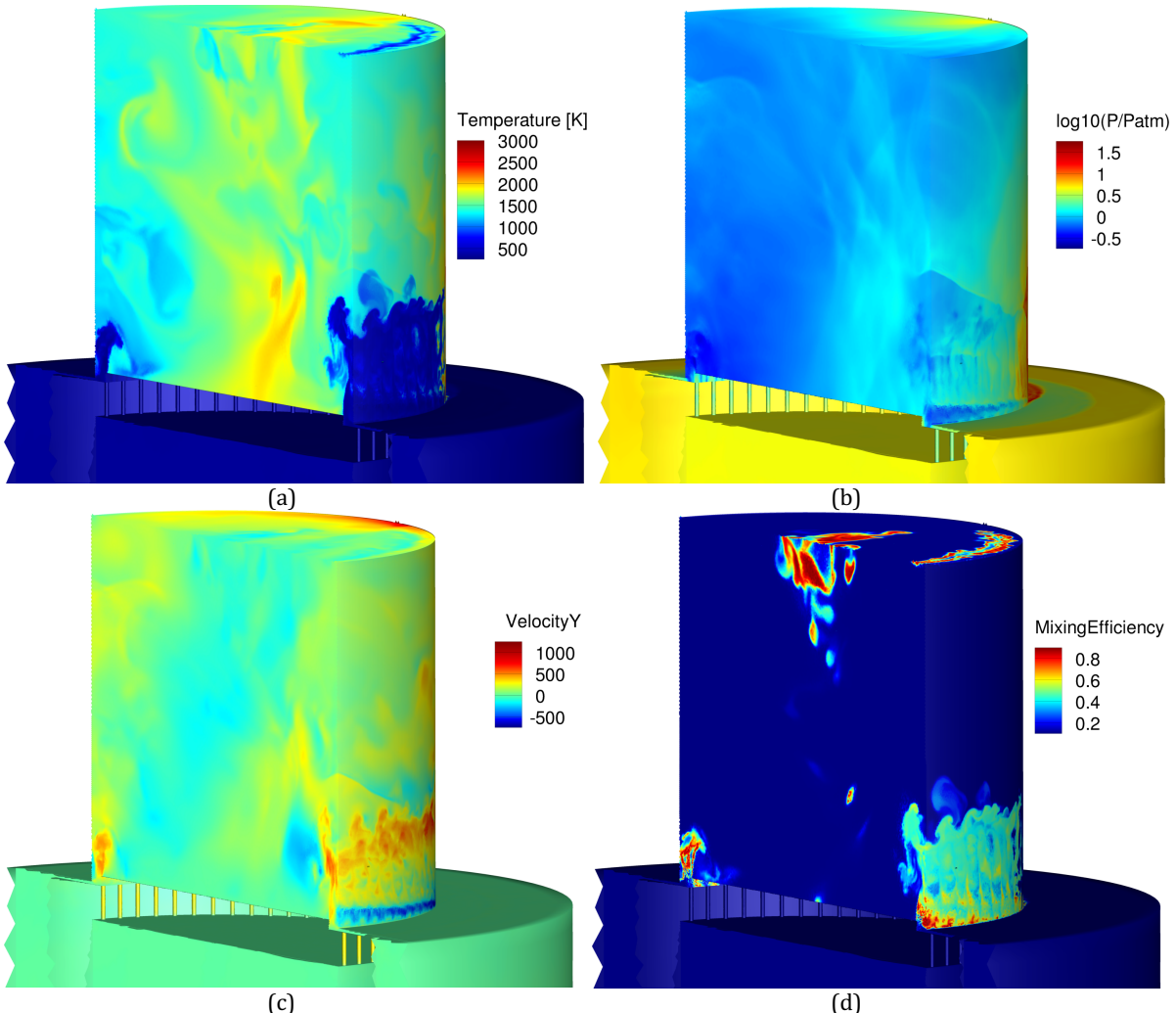


Figure 4. (a) Temperature, (b) pressure, (c) axial velocity, and (d) mixing efficiency for the hollow RDC. Same conditions as Figure 3.

The mixing efficiency (Fig. 7a) shows the best mixing is near the injectors through the entire fill zone, and then becomes less well mixed as we go up towards the top. To determine what the mixture is like higher in the mixing zone, we show the ethylene mass fraction in Figure 7b. Clearly, the mixture becomes rich as we get higher in the fill zone away from the injection face. This is most likely due to the radial injection pattern for the air inlet. Some of the air gets mixed in with the ethylene that is caught in the short, outer recirculation zone, but most of the air must be lost towards the core region.

We have already shown that core dump region is filled with hot product gases at low velocities and moderate pressures in Fig. 4. We can also examine the conditions at the plug headend wall to get a better idea of the conditions within the core, and compare these to some of our previous work.

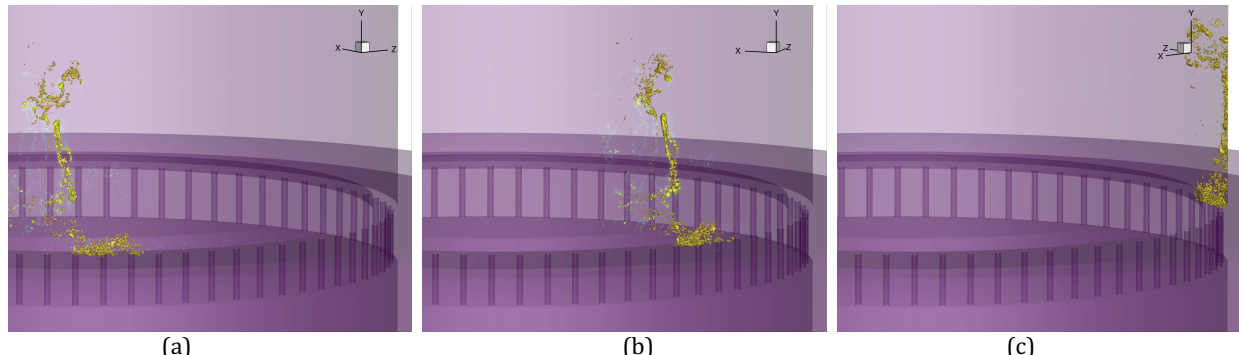


Figure 5. Heat-release surface showing shape of detonation wave from different locations for the non-premixed H-RDE simulation. Same conditions as Figure 3.

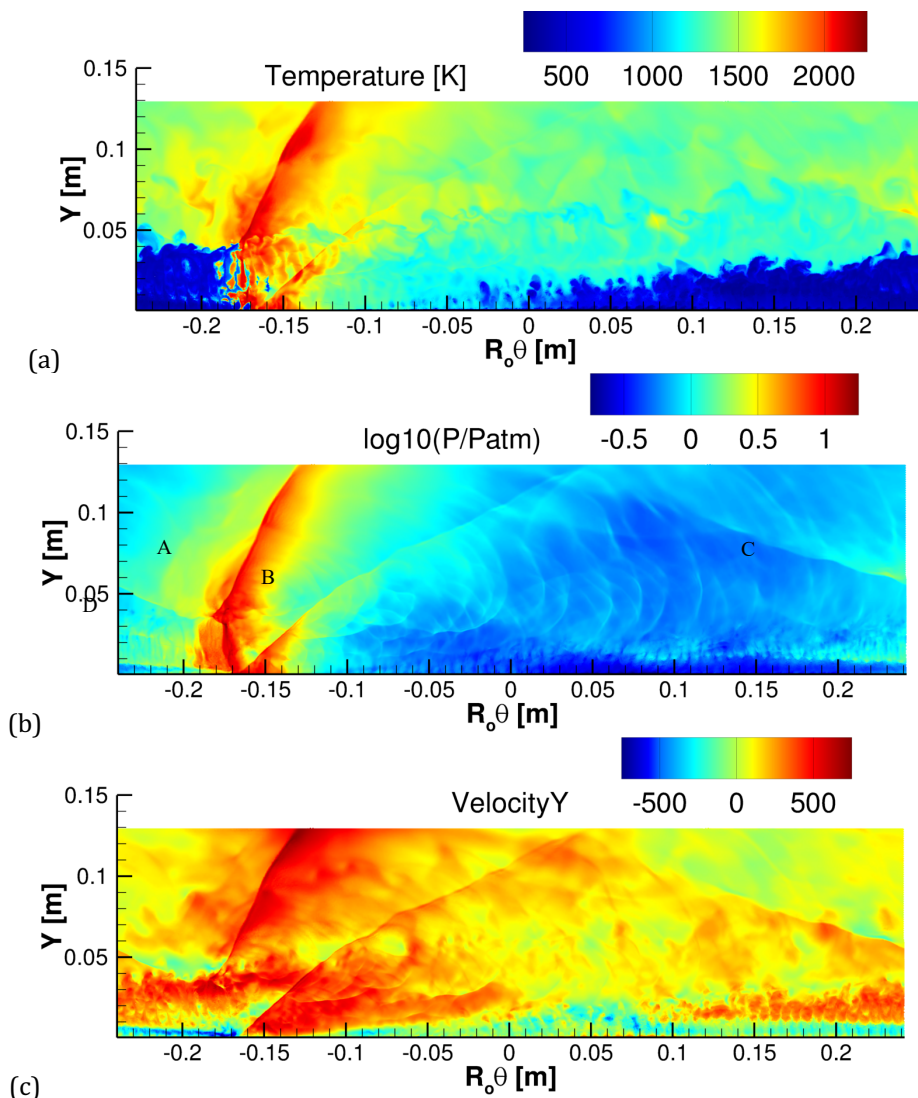


Figure 6. (a) Temperature, (b) pressure, (c) axial velocity at the unrolled combustion chamber wall. Same conditions as Figure 3.

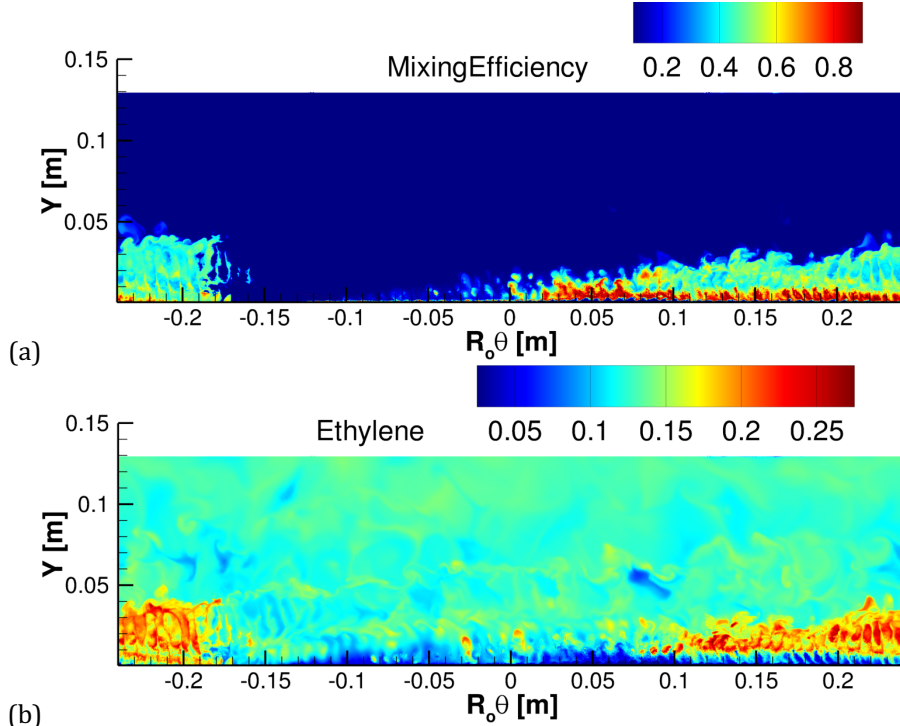


Figure 7. (a) Mixing efficiency and (b) ethylene mole-fraction at the unrolled combustion chamber wall. Same conditions as Figure 3.

Figure 8 shows the temperature, pressure, radial and azimuthal velocities at the plug wall and injector face. Because this is at the wall boundary condition, the axial or normal velocity will be zero based on the boundary condition, and so is not shown. What stands out the most in Figure 8 is that the core flow has a large area of high temperature, high pressure product gas leading the detonation wave. This was also found in the previous studies with a simplified geometry and ideal injection. Unlike the previous solution, this high pressure region (especially the high temperature area) is larger and more chaotic than found for the idea injection, and the simulation should be run further to ensure that the plug headend wall solution remains similar. Fig 8c-d shows the radial and azimuthal velocity and the plug headend wall and injector face.

Figure 9 shows the mixing efficiency at the plug wall and injector face. We are interested in determining where the mixture hits the target equivalence ratio. In the fill region away from the detonation wave, the mixture efficiency between the injectors and the plug is very close to 1. On the plug headend wall, it is mostly close to 0, because these region consists of product gases, mixed in with either just ethylene or air (since the temperature is hot enough to react any remaining mixture of both fuel and oxidizer). There are still some small pockets of unreacted mixture in the core region. Near the detonation wave, once the first wave hits the injector face, the ethylene and air quickly becomes perfectly mixed, causing the trailing combustion and second reflected wave as seen in Figs. 5 and 6b. A closeup of this is shown in Fig. 9b.

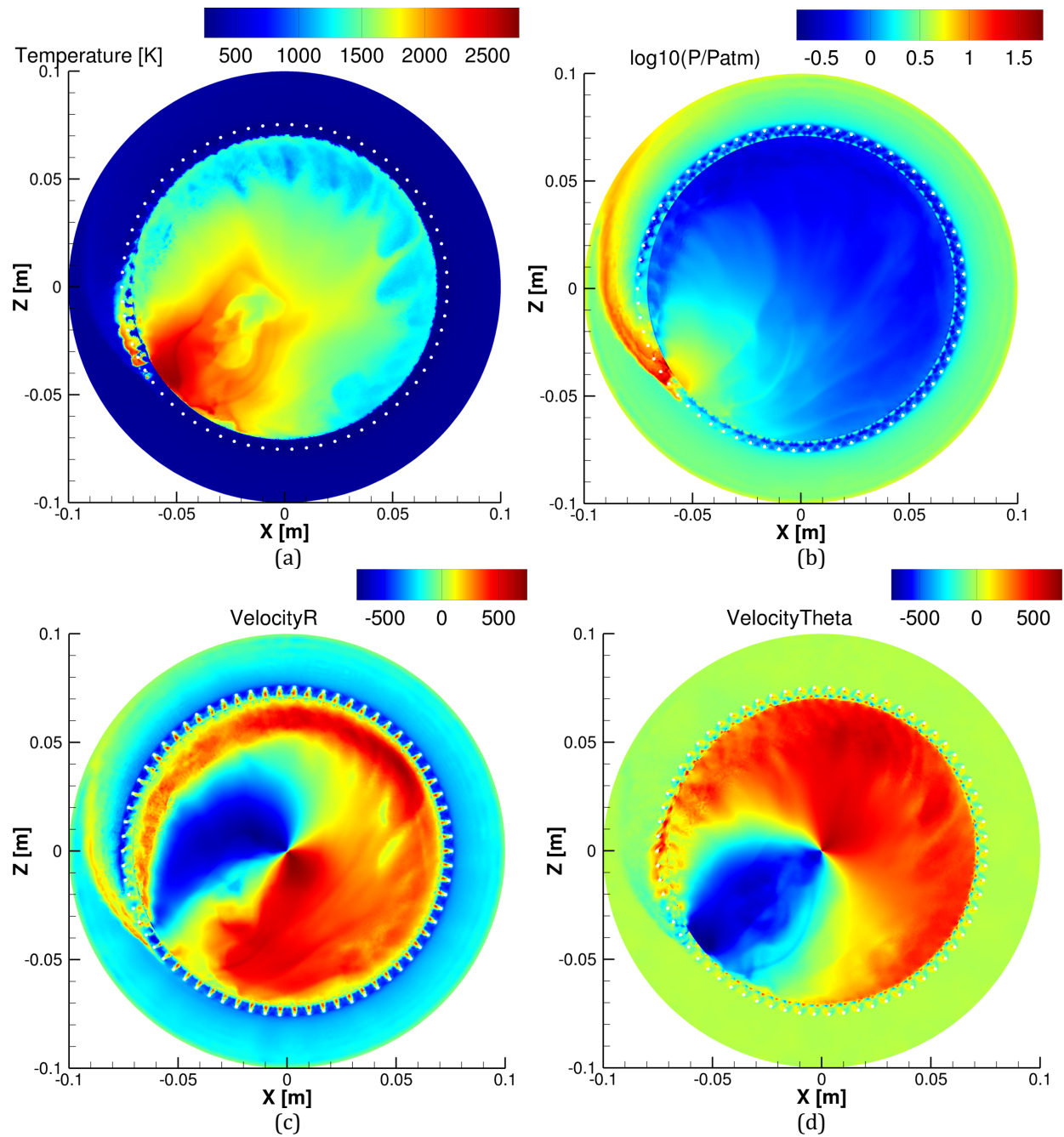


Figure 8. (a) Temperature, (b) pressure, (c) radial velocity, and (d) azimuthal velocity at the plug wall and injection face. $\dot{m} = 0.647 \text{ kg/s}$, $\phi = 1.16$.

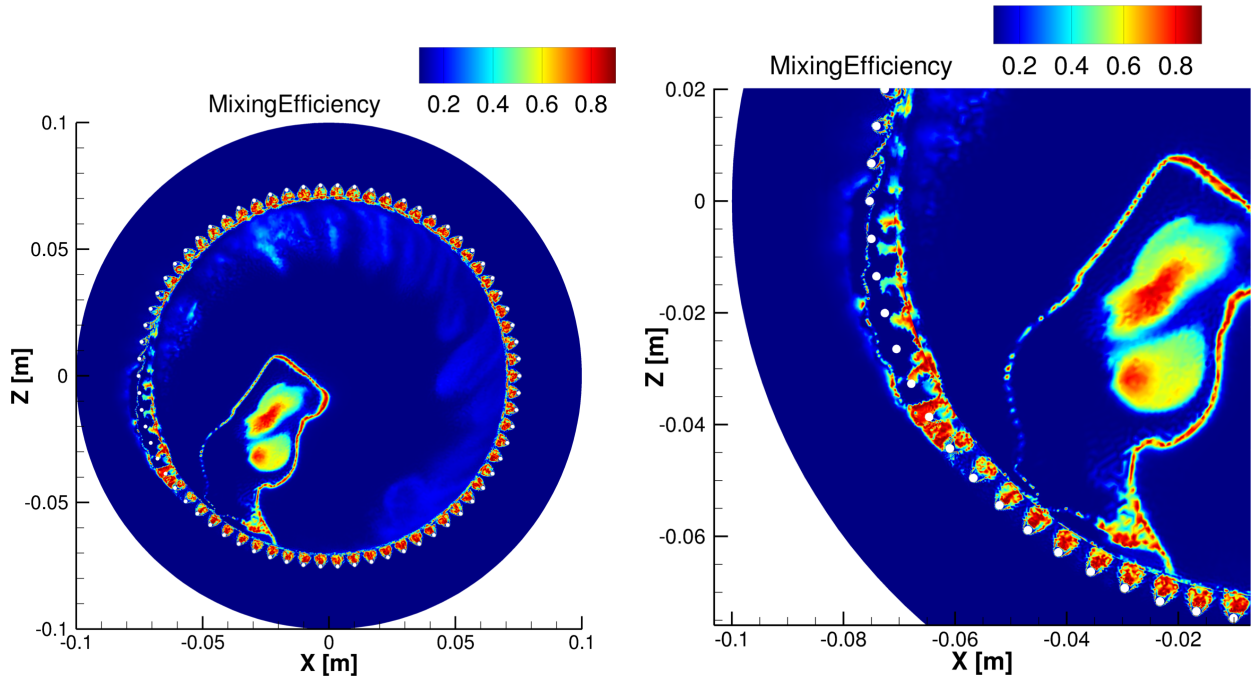


Figure 9. Plug wall and injection face. $\dot{m} = 0.647 \text{ kg/s}$, $\phi = 1.16$.

V. Summary and Conclusions

This paper builds on our previous work with centerbody-less combustors^{7,8} to look at the detonation dynamics that are associated with centerbody-less RDCs, and begin to compare them with what is known about annular RDCs. The simulations are grounded in experiments conducted at the University of Cincinnati. The non-premixed hollow RDC simulation showed a stable detonation running an ethylene/air mixture with a mass-flow rate of 0.647 kg/s and an equivalence ratio of 1.12. Results showed the injection pattern produced two recirculation zones, a small one near the injectors on the outside wall, and a second recirculation zone further into the fill region. Three regions of heat-release related to the detonation wave were identified: the upper portion of the detonation wave, which was the strongest with heat release extending slightly into the interior of the domain, a region that hugged the wall and showed a somewhat corrugated presentation on the outer wall due to the discrete fuel injection, and a third region near the injectors that lagged the other two. The presence of strong heat-release lagging the main detonation wave resulted in an additional reflected shock wave running parallel to the oblique shock wave from the top of the detonation, which was consistent with earlier simulations using an ideal injection model. This solution demonstrated the potential of simulations to help understand the dynamics underlying hollow RDCs. Additional simulations should be run to examine how the dynamics change at different flow-rates and equivalence ratios, and more detailed kinetic models can be used to better capture the deflagration occurring in the fill zone.

Acknowledgments

This work is supported by the Office of Naval Research under the Sea Based Aviation program, and by the Air Force Office of Scientific Research and AFRL. The authors would also like to thank the Andrew Corrigan, Andrew Kercher, and David Kessler for their help with running JENRE® on different platforms and with diagnostics.

References

- ¹Zhou, R., Wu, D., Wang, J., "Progress of continuously rotating detonation engines," *Chinese Journal of Aeronautics*, Vol. 29, Iss. 1, 2016, pp 15-29.
- ²Xin-Meng Tang and Jian-Ping Wang and Ye-Tao Shao. "Three-dimensional numerical investigations of the rotating detonation engine with a hollow combustor," *Combustion and Flame*, V. 162, Is. 4, p 997 – 1008, 0010-2180, 2015.
- ³Songbai Yao, Xinmeng Tang, Mingyi Luan, and Jianping Wang. "Numerical study of hollow rotating detonation engine with different fuel injection area ratios," *Proc Combust Inst*, V. 36, Is. 2, p 2649 - 2655, 2017.
- ⁴W. Stoddard, E.J. Gutmark, "Numerical investigation of centerbodiless RDE design variations," AIAA 2015-0876, AIAA SciTech Forum 2015.
- ⁵W. Stoddard, A. St George, R. Driscoll, V. Anand, E. Gutmark, "Experimental Validation of Expanded Centerbodiless RDE Design," AIAA 2016-0128, AIAA SciTech Forum 2016.
- ⁶Anand, V., St. George, A., de Luzan, C.F., and Gutmark, E., "Rotating detonation wave mechanics through ethylene-air mixtures in hollow combustors, and implications to high frequency combustion instabilities," *Experimental Thermal and Fluid Science*, Vol. 92, pp. 314-325, 2018.
- ⁷Schwer, D.A. and Johnson, R., "Numerical Investigation of Centerbody-less Rotating Detonation Combustors," AIAA Paper 2020-2158, AIAA SciTech Forum, 6-10 Jan 2020, Orlando, FL.
- ⁸Schwer, D.A., Corrigan, A., and Kailasanath, K., "Toward Efficient, Unsteady, Three-Dimensional Rotating Detonation Engine Simulations," AIAA Paper 2014-1014, AIAA SciTech Forum, 13-17 Jan 2014, National Harbor, MD.
- ⁹Schwer, D.A., Johnson, R., Kercher, A., Kessler, D.A., and Corrigan, A., "Progress in Efficient, High-Fidelity Rotating Detonation Engine Simulations," AIAA Paper 2019-2018, AIAA SciTech Forum, 7-11 Jan 2019, San Diego, CA.
- ¹⁰Liu, J., Corrigan, A., Kailasanath, K., Ramamurti, R., Heeb, N., Mundary, D., and Gutmark, E. "Impact of Deck and Jet Blast Deflector on the Flow and Acoustic Properties of Imperfectly Expanded Supersonic Jets," AIAA Paper 2013-0323, 51st AIAA Aerospace Sciences Meeting, 2013.
- ¹¹Gottlieb, S., Shu, C., and Tadmor, E., "Strong stability-preserving high-order time discretization methods," SIAM review, Vol. 43, No. 1, 2001, pp. 89–112.
- ¹²Corrigan, A., Kercher, A., and Kessler, D., *A Moving Discontinuous Galerkin Finite Element Method for Flows with Interfaces*, Memorandum Report, NRL/MR/6040—17-9765, U.S. Naval Research Laboratory, 2017.
- ¹³Schwer, D.A. and Kailasanath, K., "Towards Non-premixed Injection Modeling of Rotating Detonation Engines," AIAA Paper 2015-3782, Propulsion and Energy Forum, 27-29 July 2015, Orlando, FL.
- ¹⁴Schwer, D.A. and Kailasanath, K., "Towards an Assessment of Rotating Detonation Engines with Fuel Blends," AIAA Paper 2017-4942, Propulsion and Energy Forum, 10-12 July 2017, Atlanta, GA.
- ¹⁵Johnson, R.F., Goodwin, G.B., Kercher, A., Corrigan, A. and Chelliah, H.K., "Discontinuous-Galerkin Simulations of Premixed Ethylene-Air Combustion in a Cavity Combustor," AIAA Paper 2019-1444, AIAA SciTech Forum, 7-11 Jan 2019, San Diego, CA.
- ¹⁶The MPI Forum, "MPI: A Message-Passing Interface Standard," July 2011, retrieved from <http://www.mpi-forum.org/docs/mpi-2.2/mpi22-report.pdf>.
- ¹⁷Karypis, G. and Schloegel, K. "ParMETIS: Parallel Graph Partitioning and Sparse Matrix Ordering Library, Version 4.0," August 2011, retrieved from <http://glaros.dtc.umn.edu/gkhome/metis/parmetis/overview>.
- ¹⁸Hoberock, J. and Bell, N., "Thrust: A Parallel Template Library," 2011, Version 1.4.0.
- ¹⁹Bell, N., and Hoberock, J., "Thrust: A Productivity-Oriented Library for CUDA," *GPU Computing Gems: Jade Edition*, Morgan Kaufmann, 2011, pp. 359-372.
- ²⁰Schwer, D.A., Kailasanath, K., and Kaemming, T. "Pressure characteristics of a ram-RDE diffuser," *Aerospace Science and Technology*, Vol 85, pp. 187-198, Feb. 2019, doi: 10.1016/j.ast.2018.11.006